Braz J Phys (2011) 41:275–280
DOI 10.1007/s13538-011-0045-y

GENERAL AND APPLIED PHYSICS

Combination of Raman, Infrared, and X-Ray Energy-Dispersion Spectroscopies and X-Ray Diffraction to Study a Fossilization Process

Francisco Eduardo de Sousa Filho · João Hermínio da Silva · Antônio Álamo Feitosa Saraiva · Deyvid Dennys S. Brito · Bartolomeu Cruz Viana · Bruno Tavares de Oliveira Abagaro · Paulo de Tarso Cavalcante Freire

Received: 24 June 2011 / Published online: 20 September 2011

Abstract X-ray diffraction was combined with X-ray energy-dispersion, Fourier-transform infrared, and Raman spectroscopies to study the fossilization of a Cretaceous specimen of the plant *Brachyphyllum castilhoi*, a fossil from the Ipubi Formation, in the Araripe Sedimentary Basin, Northeastern Brazil. Among the possible fossilization processes, which could involve pyrite, silicon oxide, calcium oxide, or other minerals, we were able to single out pyritization as the central mechanism producing the fossil, more than 100 million years ago. In addition to expanding the knowledge of the Ipubi Formation, this study shows that, when combined with other experimental techniques, Raman spectroscopy is a valuable tool at the paleontologist's disposal.

F. E. de Sousa Filho
Departamento de Física, Universidade Regional do Cariri,
Crato-CE, Brazil

F. E. de Sousa Filho · B. T. de Oliveira Abagaro · P. de Tarso Cavalcante Freire (✉)
Departamento de Física, Universidade Federal do Ceará,
Fortaleza-CE, Brazil
e-mail: tarso@fisica.ufc.br

J. H. da Silva
Universidade Federal do Ceará—Campus do Cariri,
Juazeiro do Norte-CE, Brazil

A. Á. Feitosa Saraiva · D. D. S. Brito
Departamento de Ciências Biológicas,
Universidade Regional do Cariri,
Crato-CE, Brazil

B. C. Viana
Departamento de Física, Universidade Federal do Piauí,
Teresina-PI, Brazil

Keywords Raman spectroscopy · Infrared spectroscopy · X-ray diffraction · Fossil

1 Introduction

Fossilization is a process affecting plant remains and animal parts buried through deposition and erosion, or even cataclysms, in sedimentary environment. In most cases, the organism is rapidly buried in an oceanic or fluvial flood, or as the result of an earthquake. If the environment is poor in oxygen and bacteria, while the water surrounding the organism is rich in minerals, the latter will substitute the original tissue and form the fossil. In other words, fossilization is a chemical–geological process that turns parts of a prehistoric animal or plant into stone [1].

We have studied fossilization in a Cretaceous sedimentary material aged around 100 million years with various physical techniques. In this paper we discuss a fossil from the Ipubi Formation of the Araripe Sedimentary Basin, in Northeastern Brazil. Fossilization most commonly involves calcination, pyritization, or silification [1]. Different processes typically occur in different regions, but in even a relatively small region, diverse fossilization mechanisms can be identified.

To study such mechanisms, a number of techniques are available, structural and vibrational analyses, among others. Raman spectroscopy, which has served several areas of knowledge, such as chemistry, physics, pharmaceutical and industrial analysis, biology [2, 3] and, in the last years, forensic science, art restoration, conservation science, art history, and archeology [4], has even more recently been applied to paleontology [5, 6].

Archeology deals with human artifacts produced 10^2–10^4 years ago. Among archeological studies one finds

investigations of dyes and pigments [7], glasses, glazes and ceramics [8], and artifacts in a general way [4]. Paleontology, by contrast, deals with fossils, aged between 10^4 and 10^8 years, and has broader scope, including prehistoric life, the paleoenvironment, the evolution of organisms, and the sequence of chemical events producing fossils.

In the Araripe Basin, one of the world's richest Cretaceous sites, most of the fossils were calcined [9]. In this region, sediments were deposited in the Cretaceous period, in a timespan of approximately 50 million years; laminated limestones, gypsite benches, shales, and fine sandstones can be found there. Among the several stratigraphic layers of the Araripe Sedimentary Basin is the Ipubi Formation, a geological unit composed of anhydrite and evaporate deposits interbedded by dark lutites [10]. The Ipubi Formation and other Formations of the Araripe Basin are shown in Fig. 1. In this unit many fossil specimens have been found, such as fishes, turtles, plants, and microfossils. Nonetheless, few aspects of the fossilization process in the Ipubi Formation have been reported. In an attempt to fill this gap, we have combined Raman spectroscopy with Fourier-transform infrared spectroscopy (FTIR), X-ray diffraction measurements, and X-ray energy-dispersion spectroscopy to analyze a fossil of the Ipubi Formation. Applied to a plant fossil, these four experimental techniques identify one of the fossilization processes in the Ipubi Formation. The results clearly indicate that pyritization played an important role in the Araripe Basin, one of the most important sites of Cretaceous fossils.

2 Experimental

The material, a fossil of the plant *Brachyphyllym castilhoi*, was collected in the Pedra Branca Mine, within the calcium sulfate excavation area close to the city of Santana do

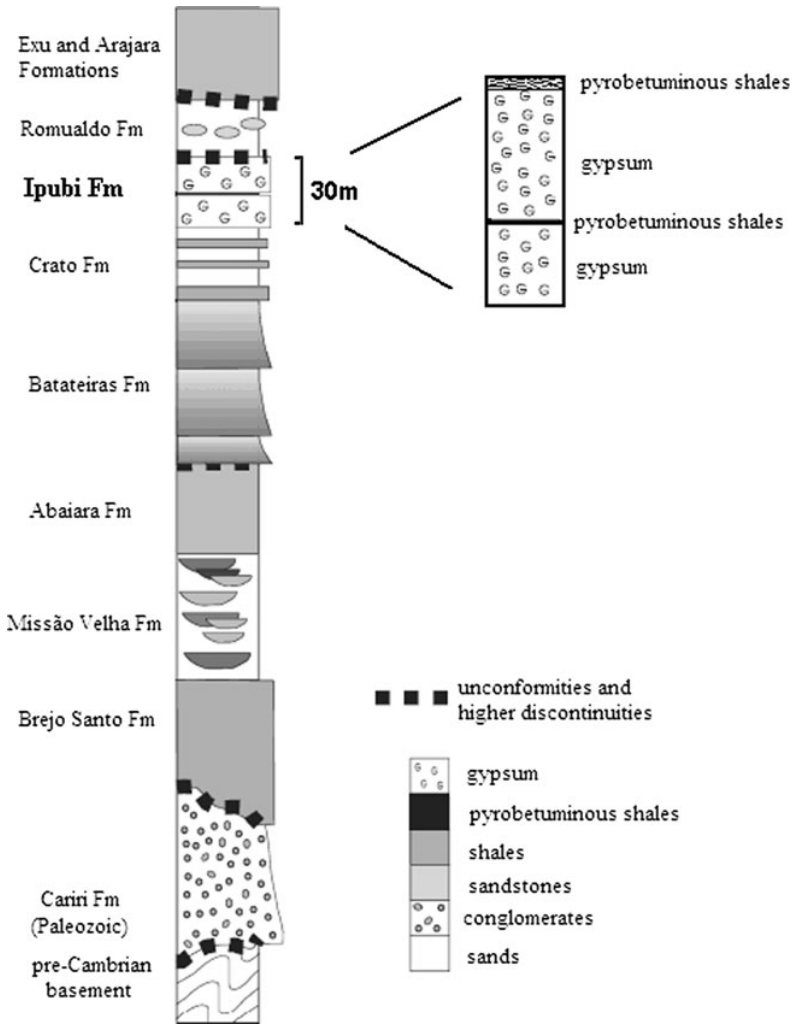

Fig. 1 Representation of the several Formations of Araripe Sedimentary Basin. The Ipubi Formation (*Fm*), in particular, is a thin layer of about 30 m in height almost at the top of the Araripe Basin

Cariri, in the State of Ceará. The sedimentary matrix is a dark-gray laminate, pyro-bituminous shale, from the level just above the gypsum-evaporate bed. At this level, many fossil impressions of fishes and plants are observed, as described by Saraiva et al. [9]. The X-ray diffraction (XRD) measurements were made in a Rigaku equipment, model DMAXB, with Bragg-Brentano focal geometry. Each sample was scanned at 1° steps per minute. The FTIR transmission spectra were measured with a Bruker spectrometer, model Vertex 70, in the 400–4,000 cm^{-1} interval. The samples were mixed with KBr around the 1:100 ratio and pressed in laminated form. The X-ray energy-dispersion spectra (EDS) were recorded in a Bruker spectrometer, model Xflash, attached to a TESCAN scanning electronic microscope, model Vega XMU. The measurements were made in vacuum, with electron acceleration energy of 30 kV allowing analysis in the energy range 0–40 keV. The Raman spectra were obtained in a triple-grating spectrometer Jobin-Yvon T64000 equipped with a N_2-cooled charge-coupled device detection system. The 514.5-nm line of an argon ion laser was used for excitation, an Olympus microscope lens with focal distance f=20.5 mm and numerical aperture NA=0.35 focusing the beam on the sample surface. The spectrometer slits were set for a resolution of 2 cm^{-1}, the laser power at the sample was set at approximately 2 mW, and the recording time at 60 s with five accumulations per spectrum segment.

3 Results and Discussion

In order to understand the results, it is important to keep in mind that the data come from a fossil, the plant *B. castilhoi*, extracted from a sedimentary rock, the matrix. Figure 2 shows the FTIR spectra of both the fossil (bottom panel) and the matrix (upper panel). The fossil spectrum shows two modes with peaks close to 1,630 and 3,437 cm^{-1}, which we associate with the O–H vibrations of adsorbed water. In addition, the fossil spectrum displays modes in the 400–420 cm^{-1} region, which we assign to the Fe–S vibrational mode and associate with pyrite (FeS_2) [11–14]. We recall that pyrite, the most abundant of metal sulfides, is found in many a geological environment [14]; nonetheless, absolutely scarce evidence has hitherto been found of its presence in the Araripe Basin fossils. The assignment of the bands around 420 cm^{-1} is confirmed by the Raman spectroscopic results, as discussed below.

Peaks at 467 cm^{-1} in the spectrum of the fossil and at 468 cm^{-1} in the spectrum of the matrix can be associated with the bending of the Si–O–Si unit in, for instance, the SiO_2 species [15]. This indicates that the fossil and matrix contain other minerals. The peak at 526 cm^{-1} is assigned to Al–Si–O bending [15–17], possibly due to aluminosilicate crystalline structures. The occurrence of silicates and aluminosilicates in both samples is confirmed by other

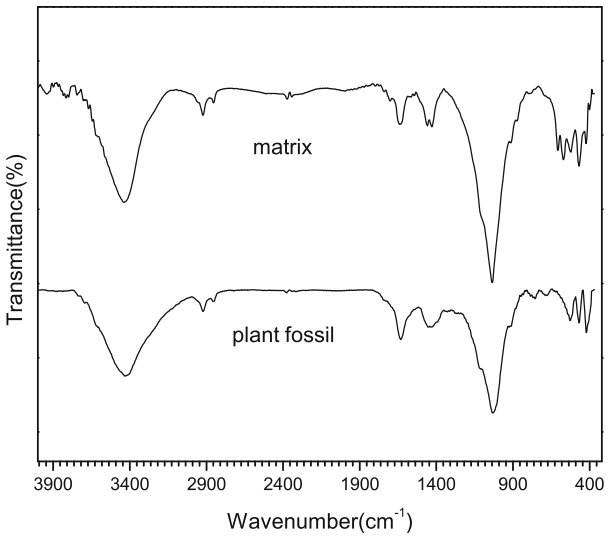

Fig. 2 FTIR spectra of the fossil (*bottom curve*) and of the matrix (*upper curve*)

peaks in the FTIR spectra, such as the one at 692 cm^{-1}, which we associate with Si–O bending, and the peaks at 878 and 911 cm^{-1} in the fossil spectrum, which we associate with Al–OH stretching [16]. Stretching vibrations of Si–O–Si [15–17] were observed at 1,024 and 1,032 cm^{-1} in the IR spectra of the fossil and matrix, respectively, while a band at 1,120 cm^{1} is associated to a bending of the Si–O unit [15]. Finally, the IR spectra of both the fossil and the matrix show vibrations between 3,600 and 3,735 cm^{-1}, which we associate with Si–OH stretching. Again, these peaks points to the occurrence of silicates—olivine, epidote, tourmaline, pyroxene, micas, and feldspars, among other possibilities. A few modes with even lower intensities are additionally visible, which can be related to small quantities of other organic and inorganic materials. Chiefly important, nevertheless, is the conclusion drawn from comparing the intensities of the peaks due to the various phases in the fossil, which indicates that the dominant phase is pyrite. Table 1 summarizes the assignment of the peaks in the FTIR spectra of the fossil and matrix.

Raman spectroscopy provides further insight into the constitution of the fossil. Figure 3 displays the Raman spectra of the plant fossil, collected from three different regions (A, B, and C), in the 40–500 cm^{-1} range. We are particularly interested in the 330–450 cm^{-1} range, where we expect to find Raman bands associated with S–S vibrations; in other words, the peaks in this region are the signature of pyrite. While infrared spectroscopy is sensitive to Fe–S vibrations, Raman spectroscopy is sensitive to S–S vibrations. Since the two vibrations are expected to coexist in the pyrite crystal, we see that the combination of Raman and IR spectroscopies unequivocally detects FeS_2 crystals in the sample.

Table 1 Measured IR active frequencies of modes appearing in the FTIR spectra of both the fossil and the matrix, and the tentative assignment

Plant fossil	Matrix	Assignment
399	400	Fe–S
406	–	Fe–S
420	422	Fe–S
467	468	Si–O–Si bending
513	–	
526	521	Al–Si–O bending
–	570	
–	606	
677	669	
692	694	Si–O bending
704	–	
–	837	Al–OH stretching
878	872	Al–OH stretching
911	911	Al–OH stretching
1,024	1,032	Si–O–Si stretching
1,120	1,112	Si–O bending
3,616	3,620	Si–OH stretching
–	3,644	Si–OH stretching
3,690	3,667	Si–OH stretching
3,735	3,700	Si–OH stretching

As explained, the Raman-active modes of pyrite depend only on movements of the S atoms; the wavenumbers give information on the vibrational motions (stretching and libration) of the S–S units [18]. The A and B spectra show bands at 342 and 377 cm^{-1}, assigned to S–S libration and S–S stretching, respectively. The weak band at 428 cm^{-1} is a coupled S–S libration and stretching vibration [18, 19]. The C spectrum presents the same bands, broadened, reduced in intensity, and shifted to 343, 378, and 432 cm^{-1}; it can thus be associated with a distorted pyrite crystal structure. The vibrations associated to pyrite crystal indicate that FeS_2 composes different regions of the plant fossil and confirms our interpretation of the FTIR spectra.

The C spectrum in Fig. 3 also shows a band centered around 470 cm^{-1}, comprising two peaks: one at 467 cm^{-1} and the other, more intense, at 472 cm^{-1}. These peaks were assigned to the Si–O–Si bend of quartz (SiO_2) [20] and to the Al–O–Si bend characteristic of aluminosilicates, such as kaolin [20, 21]. Low-intensity peaks close to 470 cm^{-1} are also visible in the A and B spectra. Additional evidence indicating the presence of quartz is provided by the band around 245 cm^{-1} (Si–O bend [20]). A weak band around 222 cm^{-1} (B spectrum) and more intense one at 218 cm^{-1} (C spectrum) were assigned to Fe–O bend vibration [20, 22]. In the B spectrum, the band at 320 cm^{-1} can be associated with an OH bend [20, 21]; this identifies a small quantity of a hydroxylated aluminosilicate mineral, for example, kaolin or other kind of hydroxy/hydrated phase, such as gibbsite (γ-$Al(OH)_3$), bayerite (α-$Al(OH)_3$), or diaspore (α-AlOOH) [23]. Thus, Raman spectroscopy attests to the conclusion drawn from the FTIR spectra: while several phases are present in the fossil, pyrite is dominant.

We were unable to record Raman spectra for the matrix, because its luminescence is too high. In an effort to further substantiate our interpretation of the FTIR and Raman spectra, we carried out EDS and X-ray diffraction measurements. EDS yields qualitative information on the chemical composition of the samples. Figure 4 presents the EDS spectrum of the fossil, which clearly indicates that Fe and S are the most abundant elements and hence confirms the results of infrared and

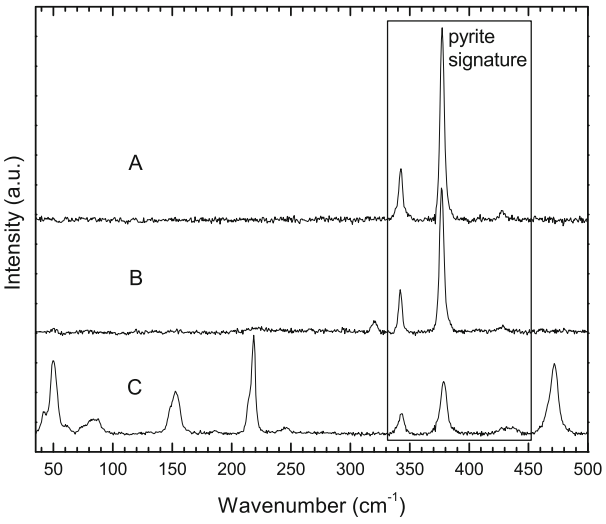

Fig. 3 Raman spectra of the plant fossil sample, obtained from different regions (*A*, *B*, and *C*) of the specimen

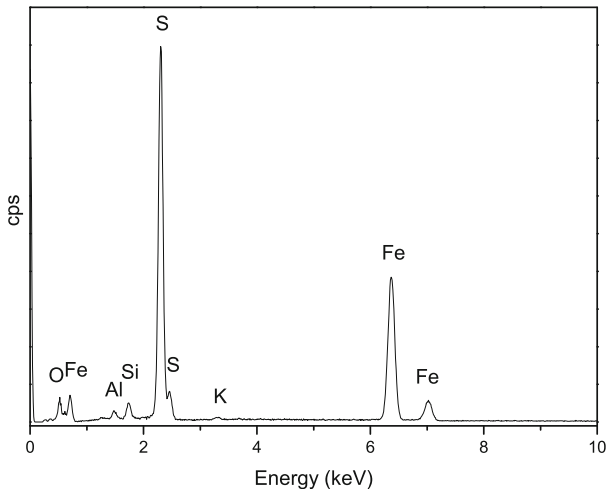

Fig. 4 X-ray energy-dispersion spectrum (EDS) of the fossil

Raman spectroscopies. Besides these elements, which form pyrite, the spectrum shows smaller amounts of K, Si, Al, and O. The latter indicate that, during the long timespan in which the material remained in liquid, anoxic environment, minerals were precipitated from the very hot waters surrounding the specimen and substituted the original content of the plant. This hypothesis is corroborated by the existence of a layer of calcium sulfate dihydrate (gypsum), with 30-m average thickness, in the place where the fossil was found. The gypsum is covered by a layer of pyrobetuminous shales and argillites containing fossils of vertebrates, invertebrates, algae, and plants.

For comparison, Fig. 5 shows the EDS spectrum of the sedimentary matrix. The larger concentration of the elements Si, Al, and O confirms the presence of aluminosilicate minerals. Smaller quantities of Fe, Ti, Ca, K, S, and Mg can also be seen. We have also performed chemical analysis through X-ray fluorescence; the results agree with those obtained from the EDS spectra.

Figure 6 shows the X-ray diffractograms of the fossil and matrix. The fossil diffractogram shows peaks that can be identified with crystalline planes of the pyrite phase (FeS_2), whose structure is cubic and belongs to the crystallographic space group *Pa3*. The width of the fossil diffraction peaks shows that it has high crystallinity. The X-ray diffractogram of the matrix displays a large number of peaks, due to several crystalline structures. In consistency with the EDS measurements, it is evident that the crystalline phases in the fossil are different from those in the matrix. Among the matrix phases we observe silicon, pyrite, aluminum silicate, magnesium, calcium, sodium, and a few oxides, as well as minor concentrations of other phases. The X-ray diffractogram confirms that pyrite is the predominant crystalline phase in the fossil and points to quasi-total substitution of FeS_2 for the *B. castilhoi*.

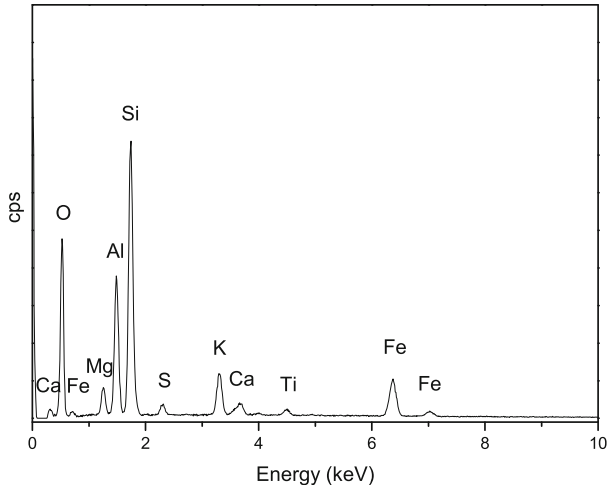

Fig. 5 X-ray energy-dispersion spectrum of the sedimentary matrix

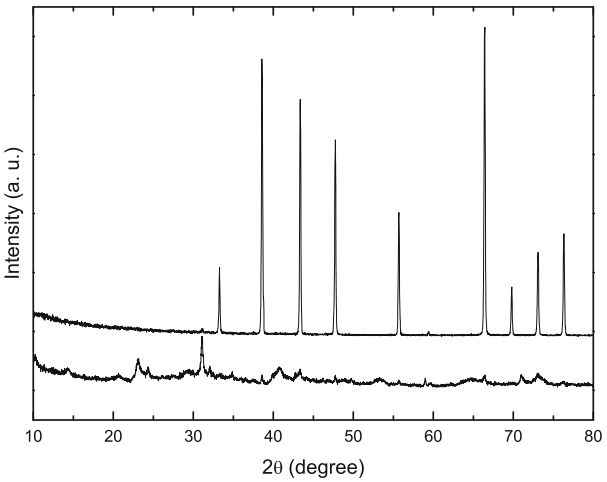

Fig. 6 X-ray diffractogram of the fossil (*upper curve*) and of the matrix (*bottom curve*)

We conclude that the *B. castilhoi* sample was pyritized, in contrast with the fossilization process of the same species in the Romualdo and Crato Formations. The geologically thin (30 m) Ipubi Formation is sandwiched between the Romualdo (above) and Crato (below) Formations. *B. castilhoi* fossils were also found in the latter two formations. While the fossils in these two units were *calcified*, the Raman, infrared, and X-ray energy-dispersion spectra in the present work shows that the fossil in the Ipubi Formation was *pyritized*. This indicates that the paleoenvironment in the Ipubi Formation is very different from the surrounding formations, both above and below.

The fossilization under paludal conditions, which are rich in sulfuric matter is, in general, a very rare event. Nevertheless, the Ipubi Formation, where pyritization plays central role, is rich in fossils. The high salinity of the environment may have favored the preservation of the fossil in the first stages of fossilization. This would indicate that, in the Creataceous period, K, Ca, and Cl formed different salts that were dissolved in water of the paleosea (or paleolake). Such a sea, or lake, subsequently underwent a high tax of evaporation and produced the gypsite ($CaSO_3$) 30-m layer below the place where the fossil was found.

Pyrite forms naturally, under marine conditions, in the 6–9 pH range [24]. Under common marine conditions at deep waters with enough oxygen, the rate of bacterial sulfate reduction and consequent pyrite formation is basically determined by the available mass of organic matter. The amount of pyrite produced by this process depends strongly on the reactivity of iron [24]. While dissolved sulfide reacts with iron oxide in few hours, in the opposite extreme, the reaction with iron-bearing silicates takes 8.4×10^4 years [25]. To estimate the time scale involved in the fossilization of the Ipubi specimens, we therefore only have to notice

that many details of the original animals or plants are preserved in the fossils. This characteristic feature of the entire Araripe Basin, where fossils are found reproducing even internal parts of animals, indicates very rapid fossilization. Thus, we are lead to conclude that, 100 million years ago, the environment was rich in iron substances easily dissolved in sulfides, that the pH of the paleosea was between 6 and 9, and that Fe occurred in the form of iron oxide.

4 Conclusions

We have combined Raman, infrared, and X-ray energy-dispersion spectroscopies with X-ray diffraction to identify a mechanism of fossilization in the Ipubi Formation. The results clearly point to pyritization of the studied plant fossil. The sample proved to be heterogeneous, with quartz and aluminosilicates probably originated from concretion of the fossil during fossilization. The abundance of sulfur and iron indicates an anoxic environment around the fossilized material during pyritization, which preserved details of the original material, allows us to estimate the pH and identifies the iron substances present in the Cretaceous period. Most importantly, on the basis of the data in Figs. 2–6, we conclude that pyritization was an important fossilization mechanism in the Araripe Basin, one of the world's most important sites of Cretaceous fossils.

Acknowledgments Authors thank CAPES, FUNCAP, and CNPq for partial financial support.

References

1. S.K. Donovan, ed. *The Processes of Fossilization*. London: Belhaven Press (1991)
2. E. Smith, G. Dent, *Modern Raman Spectroscopy: A Practical Approach* (Wiley, New York, 2005)
3. R.L. McCreery, *Raman Spectroscopy for Chemical Analysis* (Wiley, New York, 2000)
4. H.G.M. Edwards, J.M. Chalmers (eds.), *Raman Spectroscopy in Archaeology and Art History* (The Royal Society of Chemistry, Cambridge, 2005)
5. S. Bernard, K. Benzerara, O. Beyssac, G.E. Brown Jr., Geoch. Cosmoch. Acta **74**, 5054 (2010)
6. J.W. Schopf, A.B. Kudryavtsev, Geol. Today **26**, 140 (2010)
7. P. Vandenabeele, H.G.M. Edwards, in *Raman Spectroscopy in Archaeology and Art History*, ed. by H.G.M. Edwards, J.M. Chalmers (The Royal Society of Chemistry, Cambridge, 2005)
8. P. Colomban, in *Raman Spectroscopy in Archaeology and Art History*, ed. by H.G.M. Edwards, J.M. Chalmers (Cambridge, The Royal Society of Chemistry, 2005)
9. A.A.F. Saraiva, M.H. Hessel, N.C. Guerra, E. Fara, Est. Geol. **17**, 40 (2007)
10. M.R. Lima, Anais Acad. Bras. Ciênc. **51**, 545 (1979)
11. H.D. Lutz, G. Waschenbach, Phys. Chem. Min. **12**, 155 (1985)
12. A. Ennaoui, S. Schroetter, S. Fiechter, H. Tributsch, J. Mater. Sci. Lett. **11**, 1131 (1992)
13. J.L. Verble, R.F. Wallis, Phys. Rev. **182**, 783 (1969)
14. M. Blanchard, M. Alfredsson, J. Brodholt, G.D. Price, K. Wright, C.R.A. Catlow, J Phys Chem B **109**, 22067 (2005)
15. A. Tabak, B. Afsin, B. Caglar, E. Koksal, J. Col. Interf. Sci. **313**, 5 (2007)
16. M.A. Legodi, D. de Waal, Spectroc. Acta A **66**, 135 (2007)
17. P. Falaras, I. Kovanis, F. Lezou, G. Seiragakis, Clay Miner. **34**, 221 (1999)
18. A.K. Kleppe, A.P. Jephcoat, Mineral. Mag. **68**, 433 (2004)
19. H. Vogt, T. Chattopadhyay, H.J. Stolz, J. Phys. Chem. Solids **44**, 869 (1983)
20. M.A. Legodi, D. de Waal, Spectrochim. Acta A **66**, 135 (2007)
21. R.L. Frost, P.M. Fredericks, J.R. Bartlett, Spectrochim. Acta A **49**, 667 (1993)
22. H.G.M. Edwards, E.M. Newton, J. Russ, J. Mol. Struc. **550–551**, 245 (2000)
23. H.D. Ruan, R.L. Frost, J.T. Kloprogge, J. Raman Spectrosc. **32**, 745 (2001)
24. F. Brock, R.J. Parkes, D.E.G. Briggs, Palaios **21**, 499 (2006)
25. D.E. Canfield, R. Raiswell, S.H. Bottreij, Am J Sci **292**, 659 (1992)